Water Air Soil Pollut (2021) 232: 94
https://doi.org/10.1007/s11270-021-05004-7

Use of Biochar for Limiting the Pathway of Exposure and Reducing the Risk of Heavy Metal Contamination from Mines

Macdonald Ogorm Mafiana · Ian Robert Dodkins · Chimezie Gabriel Dirisu · Shi-Weng Li

Received: 20 May 2020 / Accepted: 14 January 2021 / Published online: 23 February 2021

Abstract Field-scale experiments were conducted to assess biochar's ability with and without supplements to sequester heavy metals of lead (Pb^{2+}) and zinc (Zn^{2+}) from stream water contaminated by abandoned mines. The study was conducted at the Frongoch mine watercourse site in central Wales for 1104 h (46 days). The methods employed include pyrolysis of waste *Leylandii* feedstocks at 700 °C and post-amendment ash at ratios in mass (kg/kg) 1:10, 1:35, 1:50, and 1:100 of biophos to biochar (BC) and 1:1:100 mixed biophos and cockleshell ash to biochar (CBB). The collected data were analyzed by ASTM Brunauer-Emmett-Teller (BET), XRF spectrometer, R-stat, and SPSS statistical procedures. The results showed that non-amended samples are better suitable as adsorbent materials of lead and zinc. Overall, this field study showed that 33 g/kg of lead and 30 g/kg of zinc could be sequestered by 50 g of biochar (BC) and activated carbon (AC) from the contaminated mine watercourse containing 0.62 mg/L and 15.8 mg/L of lead and zinc metals flowing at 0.014 m^3/s. These adsorbent materials BC and AC applications are variably recommended at an optimal replacement interval of 1104 h (46 days) and 72 h (3 days) for lead and zinc sorption, respectively.

Keywords Water pollution · Biochar · Lead · Zinc · Pyrolysis · Metal adsorption · Mine waste

Practitioner Points
- Post-amendment ash supplement has a significant effect on modified biochar.
- Overall, Pb^{2+} and Zn^{2+} adsorption in 46 days was 33 g/kg and 30 g/kg, using 50 g of biochar and activated carbon, respectively.
- The surface area is a mechanistic adsorption factor common to biochar and activated carbon.
- Pb^{2+} adsorption was most statistically ($p < 0.05$) correlated to K and Mg ions, while Zn^{2+} adsorption most with Mg ion, Na ion, and BET area for sorption sites.

1 Introduction

Heavy metal pollution from both natural and anthropogenic sources is toxic and persistent in the environment.

M. O. Mafiana · I. R. Dodkins
Department of Biosciences, Wallace Building, Swansea University, Singleton Park, Swansea SA2 8PP, United Kingdom

M. O. Mafiana (✉) · C. G. Dirisu
Department of Biology Education, Federal College of Education (Technical) Omoku, Omoku, Rivers state 510103, Nigeria
e-mail: donald70us@yahoo.com

S.-W. Li (✉)
School of Environmental and and Municipal Engineering, Lanzhou Jiaotong University, Lanzhou 730070, China
e-mail: lishweng@mail.lzjtu.cn

Although some metals are essential trace elements naturally found in food and water in small amounts, they can be harmful above certain limits specified by the World Health Organization (WHO 2011; J. J. Zhao et al. 2019). Bioaccumulation, high toxicity, and carcinogenic effects of heavy metals pose a threat to human health (Järup 2003). Some health implications associated with some notable heavy metals are high risks of cancer, renal and neurological effects, developmental delay, hypertension, and mental retardation (Shi et al. 2019). These health risks have raised global concerns over the last 100 years about regulating most harmful metals such as Pb, Zn, Cu, Mn, Cd, Hg, As, and Cr in domestic products (European Commission DG ENV. 2002). On the other hand, mine waste is another medium through which heavy metals find their way into waterways and finally into the food chain (Gyamfi et al. 2019; Hudson et al. 2018).

Frongoch mine near Pont-rhyd-y-groes, central Wales, was a lead and zinc mine site operated in the 1700s–1900s covering over 11 hectares of land area, which left vast waste dumps at the end of its operation (Fig. 1a). Heavy metals are discharged from the underground workings via the abandoned Frongoch Adit study site situated 52° 21′ 04.211″ N, 3° 53′ 28.612″ W. Based on the 2015 classification, Frongoch mine metal discharge majorly impacted the ecological and chemical state of Frongoch stream, Nant Cell, Nant Cwmnewydion, and the River Magwr downstream, and consequently failed to achieve the EU Water Framework Directive standards (Edwards and Williams 2016; Hudson et al. 2018). The heavy metal pollution also affected economic and recreational activities and could be poisonous to aquatic species. Among the 4908 non-coal abandoned mines on the priority list in Wales and England (Fig. 1c), Jarvis and Mayes (2012) noted that Pb, Cd, and Zn were major metal pollutants of national concern from Frongoch mine. Prior to remediation, approximately 23 and 1.5 tons of zinc and lead metals was discharged annually, which ranked Frongoch as Wales' second most polluted mine and a top priority among other mine sites (Edwards et al. 2016).

Several remediation approaches have been undertaken by the Natural Resources Wales (NRW) to minimize heavy metal flow downstream, such as stream diversion in 2011, surface drain around the mine waste and flood attenuation pond in 2013, low-permeability capping of mine waste and creation of a wetland area in 2015, and further capping in 2018 (Fig. 1b). Though these remediation strategies have yielded considerable success in immobilizing polluting metals from the mine waste and diverting watercourse, their impact is still a concern. In the monitoring data for water quality, Edwards et al. (2016) noted an 80% water flow reduction, and consequently, zinc, lead, and cadmium by 44%, 63%, and 58%, respectively. Besides the cost-intensive nature of these projects, it is imperative to clearly understand the relationship between point and diffused pollutant sources, considering the long-term metal deposits downstream along pathways into river catchments (Environment Agency 2012). However, lead and zinc metal tailings are still lingering along the watercourse path through the resuspended metal-rich sediments. Hence, there is a need for further studies on appropriate non-invasive remediation approach with minimal costs and disturbances on the catchment pollution sources (Crane et al. 2017).

Biochar is a carbon-rich, porous, and stable solid formed when pyrolyzed under limited oxygen. It is considered a promising eco-friendly and cost-effective adsorbent of heavy metals using pyrolyzed waste biomass materials. These include animal waste (J. Liu et al. 2020; W. Zhang et al. 2020), waste pine cone biomass (Biswas et al. 2020), waste crop residues (R. Xiao et al. 2019), and industrial waste materials of biosolids (Qiu and Duan 2019). The unique adsorbent properties of biochar are induced by pyrolysis heat transformation that forms a carbon-ring without oxygen or hydrogen (Hu et al. 2020; Kim et al. 2019).

Although biochar properties and adsorption efficiency of Pb^{2+} and Zn^{2+} metal have been investigated and reviewed over time in many studies (Betts et al. 2013; Li et al. 2017; L. Wang et al. 2019a), no previous on-site field study using biochar has been published on this watercourse. Unique properties of biochar vital for metal adsorption are surface chemistry (Song et al. 2020), mineral ions content (Cheung et al. 2000), pH level (Y. Xiao et al. 2017), surface area, and functional group (Inyang et al. 2016). Different biochar amendments have improved their properties to acquire optimal adsorption capability (Godwin et al. 2019). Nevertheless, Wu et al. (2019) noted that most modifications are uneconomical for broad field-scale implementation and could be another secondary pollution source. Commercial activated carbon has recorded unique adsorptive properties for heavy Pb^{2+} and Zn^{2+} metals in wastewater treatment studies attributed to having a high surface area (Loganathan et al. 2018). Compared to other

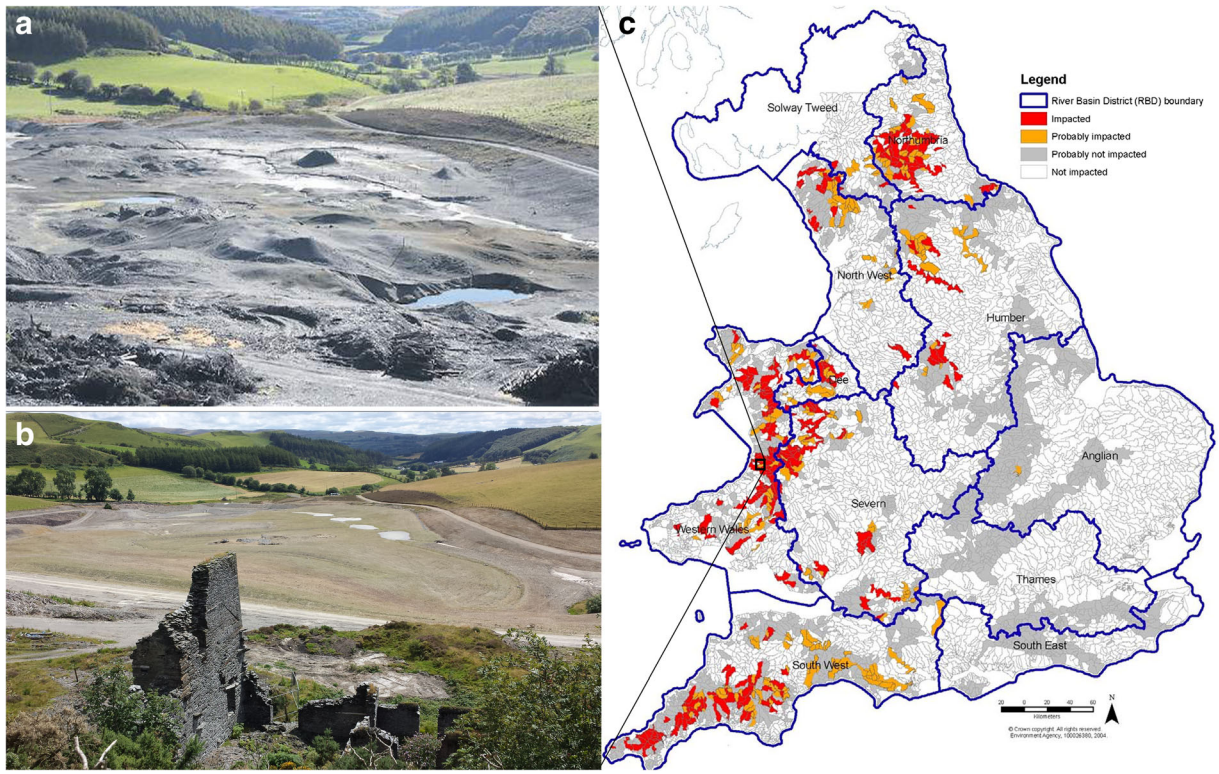

Fig. 1 Abandoned Frongoch metal mine site and its remediated state. **a** Abandoned mine ruins in 2020 (Paul Edwards 2010). **b** Impermeable capping of mine waste and creating a wetland area by NRW in 2015. **c** Heavy metal-polluted water bodies impacted by abandoned non-coal mines in England and Wales (Jarvis and Mayes 2012)

commercial metal adsorbents such as activated carbon, cactus, alumina, and silica gel (Amari et al. 2019; Rabia et al. 2018; Renu et al. 2017), biochar has enormous environmental benefits. These include but are not limited to a reduction in global warming (Ma et al. 2019), biomass-waste valorization (Foong et al. 2020), minimized agricultural waste (L. Liu et al. 2019), and economically estimated at 200% lower than activated carbon (Thompson et al. 2016). Hence, it is considered most suitable for a large-scale field application.

In a review, L. Wang et al. (2019a) noted that there is limited field application of conventional biochar on water treatment due to a relatively low metal adsorption efficiencies metals such as Cr^{6+}, As^{5+}, and Pb^{2+} (Tan et al. 2016), while other studies noted that its efficiency could vary by the nature of biomass and production processes (Boeykens et al. 2019; Kwak et al. 2019). This study carried out a field-scale application on Pb^{2+} and Zn^{2+} metal adsorption along Frongoch mine adit's watercourse. We hypothesize that pyrolyzed waste biomass of pine feedstock (*leylandii*) and activated carbon could be promising adsorbents for Pb^{2+} and Zn^{2+} heavy metal pollutants in Frongoch Adit. Hence, the objectives of this study are (1) to determine the adsorption capability of pyrolyzed waste *leylandii* feedstock in its untreated form for a possible large-scale and low-cost application and (2) to investigate the effect of post-amendments on biochar at different saturation ratios of biochar per ash supplement (kg/kg).

2 Materials and Methods

2.1 Pyrolysis and Ash Amendment

Dried mixed chips of pinewood waste (*leylandii*) feedstocks were pyrolyzed at 700 °C in a burning chamber by Sion Brackenbury pyrolysis company. After pyrolysis, a known proportion of the pyrolyzed biochar was treated with ash in a mixer and periodically sprayed with water to facilitate the binding of ash to the biochar surface. The treatment was scaled by a mass ratio (kg/kg) of supplement at saturation ratios of 1:10 (BB1), 1:35 (BB2), 1:50 (BB3), and 1:100 (BB4) of biophos ash to biochar, respectively. Another portion of biochar was amended with cockleshell

ash and biophos ash at a mass ratio (kg/kg/kg) of 1:1:100 (CBB). Commercial activated carbon (AC) and a portion of the biochar were unamended (BC), while the contaminated water was used as the study control. The samples' surface area, pH, and metal ions were determined via ASTM Brunauer-Emmett-Teller (BET) analysis, black carbon's ASTM standards (ASTM D6851 2011), and Rigaku benchtop XRF spectrometer, respectively.

Leylandii was chosen for this study because it is one of the fastest-growing native coniferous trees common in Wales and England. If a suitable metal adsorbent, it could serve as a strategy to improve its waste management. Cockleshells are wastes from harvested marine bivalve mollusks common in Wales. They contain 98% calcium carbonate ($CaCO_3$) (Moideen et al. 2020) and have been recorded as a cost-effective adsorbent of Pb^{2+} in a previous study (Budin et al. 2014). Biophos ashes are waste from Swansea power station, which was provided by Sion Brackenbury of Commons Vision Ltd. Biophos ash was tested for its adsorbent capabilities similar to other kinds of ashes reported in earlier studies such as fly ash (Novais et al. 2016), biomass ash (Xu et al. 2018), and coal ash (Shaobin Wang et al. 2006). Additionally, it contains significant Na^{+} and Mn^{+}, notable for Pb^{2+} and Zn^{2+} metal adsorption (Esrafili et al. 2019; Holguera et al. 2018). These supplements were used to alter the biochar surface and mineral ion content.

2.2 Field Experiment

The study site is located at Frongoch Adit, situated 52° 21′ 04.211″ N, 3° 53′ 28.612″ W in central Wales (near Pontrhydygroes). Fifty grams of BB1, BB2, BB3, and BB4, cockleshell-biophos supplement CBB, unamended BC, and AC samples were weighed out. Using a 1-mm sieve, the samples were filtered to remove unbounded excess ashes from the biochar and packaged in long socks of 100-μm nylon mesh filter bag to a total of 63 sample balls: 9 balls in each role of 7 socks. The sample balls were compartmentalized with plastic cable ties 2 × 140 mm, one cable tie at each sample's top and bottom, leaving 1-m space between ties. The partitioned sample socks were tied on a 10-m nylon rope attached to a wooden frame and allowed to float in the pool of metal-contaminated water of an estimated average volume of 45 L for 46 days at sampling intervals of 72, 240, 432, 624, and 1104 h (Fig. 2). Each collection was done by cutting off the last sample in each sock and taken to Swansea University in a sealed polyethylene bag for further analysis.

2.3 Sample Collection and Statistical Analysis

The collected samples were dried in labeled crucibles at 80 °C for 24 h. The dried samples were pounded with a ceramic mortar and pestle and sieved at <63 μm, as recommended for benchtop XRF analysis machine. Two grams of each sample is placed in a 24-mm XRF-labeled circumference sampling plastics cups, enclosed with 4-μm prolene film at its bottom. Each sample in three replicates was compressed with a Pana press vice at 350-in. pounds' scale and 7-mm height before enclosing with the cover and transferred to the benchtop XRF spectrometer for analysis. The water samples were collected and analyzed by NRW via inductively coupled plasma mass spectrometer (ICP-MS) and industrial and chemical measurement (ICM-QES).

The sample size consists of only three replicates per sample, suggesting a non-parametric test due to sample size. Statistical analysis was performed using a Kruskal-Wallis test in R-stat software version 3.6.1 to determine samples' statistical significance at a 95% confidence interval. Regression analysis was used to examine the correlation between sample mineral ions and metal adsorption using IBM SPSS statistics software version 25 and Microsoft Excel for graphical adsorption analysis.

3 Results and discussion

3.1 Pre-experimental Characteristics of Samples and Water Quality Analysis

The water quality result shows that zinc concentration (15.8 mg/L) was 25 times higher than lead (0.62 mg/L), while cadmium (0.02 mg/L) was considered the least among the three metals of major concern. Other parameters include ion content of sodium (Na^{+}): 6.9 mg/L, magnesium (Mg^{2+}): 4.6 mg/L, potassium (K^{+}): 1.0 mg/L, and calcium (Ca^{2+}): 16.1 mg/L; pH: 7.2; conductivity; and flow: 0.014 m^3/s (Table 1).

The samples' physicochemical properties showed variations in metal content, mineral ions, and BET surface area. BC and amended BB1–4 had a relatively equal amount of Pb^{2+}, Mn^{+}, and Zn^{2+} higher than AC. The Fe^{2+} content in AC at 958 ppm was higher than other samples by 124% than BC, 139% average than BB1–4,

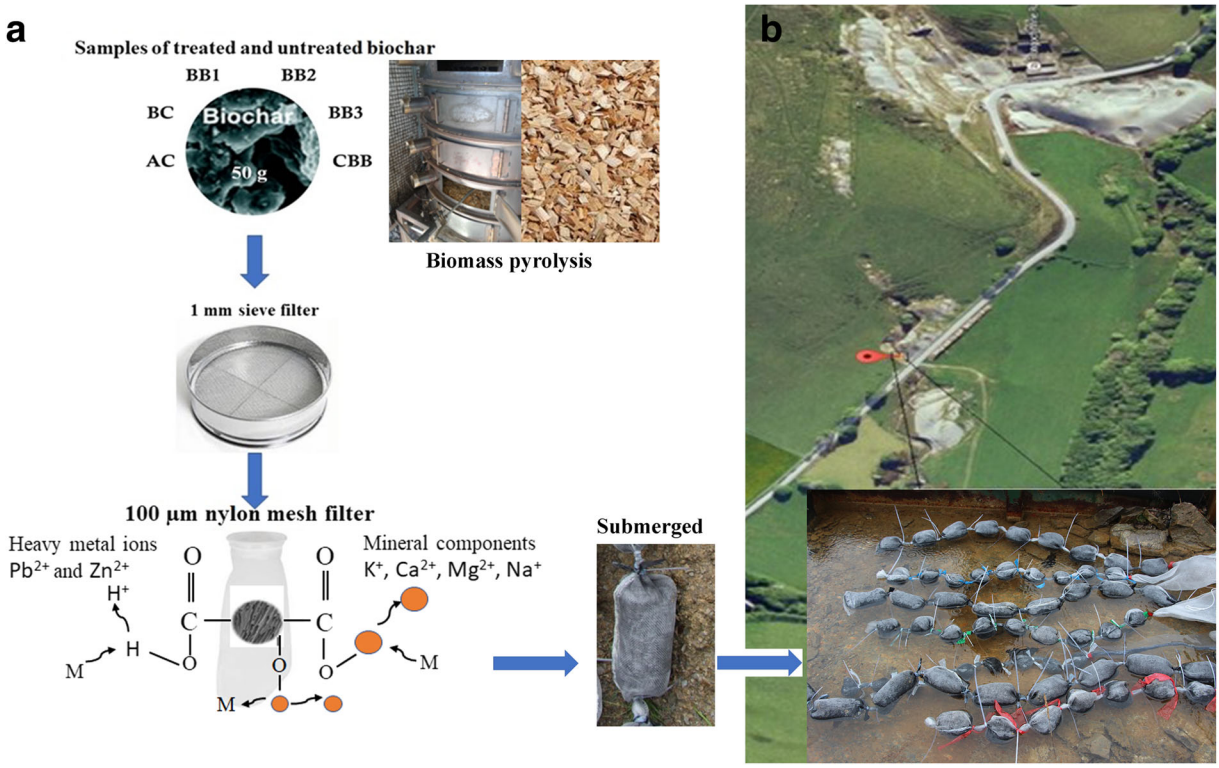

Fig. 2 **a** Schematic diagram illustrating biochar sample preparation and the mechanism of metal removal. **b** Site installation

and 46% than CBB. The mineral ion contents of K^+, Ca^{2+}, Mg^{2+}, and Na^+ suggest a variation by nature of samples and amendment supplement. No significant difference in K^+ content was shown between BC and AC but slightly differed among treated samples. CBB had more Ca^{2+} by 108% among treated samples than BB1–4, but AC had the highest Ca^{2+} content. Initial Pb^{2+} and Zn^{2+} contents in treated BB1–4 samples were low but slightly higher in Na^+ than untreated BC. The Brunauer-Emmett-Teller (BET) surface area analysis revealed that AC at 987 m^2/g was 2.7 times higher than BC and 8.3 times higher than the average of BB1–4. Comparatively, the ash amendment supplement caused a decrease in BB1–4 samples' surface area by 65% and CBB sample by 76% relative to the unamended BC (Table 2).

Similarly, a larger surface area of AC was observed by H. Wang et al. (2020), who noted that AC at 1658 $m^2\ g^{-1}$ was 96.2 times larger than the non-activated BC at 17.9 $m^2\ g^{-1}$. Biophos ash supplement had little or no significant effect on the samples' pH, which is similar to Bentley and Summers (2020) findings, who noted an insignificant effect of ash on pine biochar pH and slightly lower than AC. Other mineral ions such as Fe^{2+}, Mg^{2+}, Ca^{2+}, and K^+ were slightly affected by increasing the biophos amendment ratio (kg/kg), while Mn^+ and Na^+ were increased. Cockleshell and biophos supplement significantly increased by 1.6 g/kg and 0.38 g/kg of Ca^{2+} and Fe^{2+} content respectively in the CBB sample, which could be attributed to the 98% calcium similarly observed in cockleshell (Moideen et al. 2020), but significantly decreased its surface area.

Notable differences in mineral ions between BC and AC were a higher Ca^{2+} content in BC, while Fe^{2+} and Na^+ were higher in AC. These variations can be attributed to the differences in the feedstock and production processes between the commercially produced and conventional biochar (Yargicoglu and Reddy 2014). However, it is unclear how these properties could affect the samples' adsorbent capabilities, but cation exchange and complexation are two critical mechanisms determined by the nature of feedstock, mineral content, and pyrolysis (Lehmann and Joseph 2009; Shengsen Wang et al. 2015; J. J. Zhao et al. 2019).

3.2 Adsorption Correlation with Adsorbent Physicochemical Features

The net adsorption at 72, 240, 432, 624, and 1104 h of total sampling intervals revealed that all samples were

Table 1 Parameters of Frongoch adit contaminated water quality

Parameter	Measurement	Unit
pH	7.2	pH unit
Conductivity at 25 °C	202.3	μS/cm
Flow	0.014	m^3/s
Hardness ($CaCO_3$)	55.7	mg/L
Sodium (Na)	6.9	mg/L
Potassium (K)	1.0	mg/L
Magnesium (Mg)	4.6	mg/L
Calcium (Ca)	16.1	mg/L
Lead (Pb)	0.618	mg/L
Cadmium (Cd)	0.021	mg/L
Chromium (Cr)	0.001	mg/L
Manganese (Mn)	0.076	mg/L
Iron (Fe)	0.076	mg/L
Aluminum (Al)	0.010	mg/L
Boron (B)	0.010	mg/L
Barium (BA)	0.013	mg/L
Strontium (Sr)	0.039	mg/L
Lithium (Li)	0.100	mg/L
Copper (Cu)	0.005	mg/L
Zinc (Zn)	15.800	mg/L
Nickel (Ni)	0.017	mg/L

Water quality parameters tested by Natural Resources Wales (NRW)

good absorbent of Pb^{2+} and Zn^{2+} at different degrees (Table 3). Mineral ions such as Na^+, K^+, Ca^{2+}, and Mg^{2+} are assayed for their role in Pb^{2+} and Zn^{2+} sorption through cation exchange capacity (CEC) interaction (Li et al. 2017; Y. Wang and Liu 2017; J. J. Zhao et al. 2019), which varies by the nature of biomass and pyrolysis conditions (Mahdi et al. 2018). Other physicochemical properties which include but are not limited to pH and BET surface area are also correlated by regression analysis (Li et al. 2017; Mahdi et al. 2018).

3.2.1 Pb^{2+} Adsorption

Adsorption per unit adsorbent mass shows that BC by 2 g adsorbed 1335 ppm in 1104 h, equivalent to 1.3 g/kg, and better than AC (1.0 g/kg) in a concentration of 0.62 mg/L (Fig. 3). The total net Pb^{2+} adsorbed by 50 g of BC and AC in 1104 h field setup was 33 g/kg and 26 g/kg, respectively, from 0.66 mg/L concentration at a flow rate of 0.014 m^3/s. The optimum Pb^{2+} adsorption was between the first sampling interval of 0–240 h at the rate of 1.9 ppm/h and reduced by 63% between the third and fifth intervals. Pb^{2+} adsorption positively correlated with K^+ and Mg^{2+} at $p < 0.05$, reflecting the high K+ content notably in BC, AC, and BB4 samples, while Mg^{2+} was higher in only BC and AC samples (Fig. 4a–f). The general knowledge of heavy metal replacement of alkaline metal or earth metals such as K^+, Ca^{2+}, Mg^{2+}, and Na^+ on adsorbent surfaces and within

Table 2 Adsorbent samples physicochemical properties

Samples	Pb^{2+} (ppm)	Mn^+ (ppm)	Fe^{2+} (ppm)	Zn^{2+} (ppm)	Mg^{2+} (ppm)	Na^+ (ppm)	Ca^{2+} (ppm)	K^+ (ppm)	BET (m^2/g)	pH
BC	5.20 ± 0.17	570.39 ± 9.75	225.44 ± 5.99	45.82 ± 0.91	640.71 ± 6.22	547.14 ± 8.60	570.83 ± 13.68	3440.32 ± 19.62	372.47 ± 1.20	7.53 ± 0.43
AC	3.50 ± 0.52	15.40 ± 0.54	958.09 ± 19.58	9.48 ± 0.16	682.5 ± 18.28	1635.01 ± 9.65	229.17 ± 21.12	3322.2 ± 54.24	987.38 ± 6.48	8.01 ± 0.85
BB1	3.82 ± 2.33	663.17 ± 8.14	55.50 ± 1.25	27.54 ± 1.49	301.57 ± 6.24	603.57 ± 12.34	104.17 ± 6.73	606.67 ± 103.12	91.39 ± 3.50	5.78 ± 0.69
BB2	3.62 ± 1.33	564.43 ± 3.22	87.43 ± 5.49	29.29 ± 2.26	326.57 ± 3.30	532.02 ± 19.81	270.83 ± 9.90	772 ± 22.40	105.44 ± 3.83	6.93 ± 1.02
BB3	6.16 ± 1.12	554.23 ± 5.92	262.89 ± 2.96	47.67 ± 1.54	303.14 ± 3.38	609.14 ± 3.42	350.00 ± 5.54	824 ± 39.66	142.23 ± 2.45	6.98 ± 1.24
BB4	5.55 ± 1.62	507.05 ± 2.75	293.38 ± 1.67	42.87 ± 1.32	560.43 ± 5.62	699.43 ± 6.72	429.5 ± 17.72	3374 ± 131.26	168.27 ± 3.03	7.32 ± 1.29
CBB	5.70 ± 2.12	634.32 ± 4.67	603.41 ± 4.38	49.77 ± 3.20	291.71 ± 4.10	421.43 ± 7.78	2129.54 ± 7.43	1102.42 ± 108.79	89.12 ± 5.50	7.16 ± 0.93

Sample values are presented in mean ± standard deviation of three replicates represented as BC (untreated biochar), AC (activated carbon), and BB1-4 (treated biophos ash to biochar samples of 1:10, 1:35, 1:50, 1:100) and CBB (treated biophos ash to cockleshell ash to biochar at ratios 1:1:100)

is observable in biochar (Jiang et al. 2015; Yu et al. 2019). The Pb^{2+} adsorption difference between BC and AC can be attributed to the higher Ca^{2+} content in BC (Ca^{2+} 571 ppm), and greater open pores than the ash amended samples (BB1–4). A similar effect of initial Ca^{2+} content on Pb^{2+} adsorption was observed by Zhao et al. (2019) in a comparative adsorption potential using different biomass feedstocks. The underlying Ca^{2+} mechanism on Pb^{2+} adsorption in biochar was explained by Wu et al. (2019), who noted that $CaCO_3$ and $Ca_3(PO_4)_2$ release their inorganic anions such as CO_3^{2-}, SO_4^{2-}, and OH^- in biochar to take up Pb^{2+} by precipitation. This inorganic anion precipitation mechanism has been earlier observed using XRD analysis (Chi et al. 2017; T. Zhang et al. 2017). Contrarily, among treated samples, Ca^{2+} did not positively correlate with Pb^{2+} or Zn^{2+} adsorption due to the highly reduced surface area that provides sorption sites. The hindered surface area's effect is most reflected in CBB (760 ppm) with the least BET and sorbed Pb^{2+}, despite its high Ca^{2+} content. Adsorbent's BET surface area is known to greatly determine the pore structure, volume, and diameter, which provides the needed sorption sites for cationic exchange capacity (CEC) (Fahmi et al. 2018). Besides other factors, ash content has been reported to significantly disrupt biochar surface area, porosity, and functional groups (Fahmi et al. 2018).

Generally, treated samples' adsorption exponentially increased by their increasing surface area (BB1 > BB2 > BB3 > BB4 > CBB), while the most treated BB1 and CBB samples were the least adsorbents of Pb^{2+}. However, there was no statistically significant difference in overall net adsorption (Kruskal-Wallis chi-squared = 2.6818, df = 6, p value = 0.8476) and between treated samples (Kruskal-Wallis chi-squared = 0.42771, df = 4, p value = 0.9801). This result suggests that besides Ca^{2+} content, the surface area is vital for Pb^{2+} adsorption.

In a laboratory batch experiment, Z. Liu and Zhang (2009) recorded a total of 4.25 mg/g Pb^{2+} adsorption using untreated pinewood biochar, while J. Zhang et al. (2019) used KOH-activated sludge biochar to sorb 57.48 mg/g. The higher adsorption capability is attributed to increased BET surface area. Using a Fe^{2+}-coated bamboo biochar, Zhang et al. (2013) achieved 298.7 m^2/g BET, which is lower than that of the *Leylandii* pinewood in this study. However, chemical modification of biochar is relatively not feasible in a field application due to cost-intensiveness. Also, Li et al. (2017), in a study by Godwin et al. (2019), noted that there were few reported field applications of biochar to remove heavy metals from contaminated discharged water, which has shown to be a promising adsorbent in this study.

Adsorption rate with contact time in all samples BC, AC, BB1–4, and CBB shows that BC adsorbed 80% of its net total Pb^{2+} in 26 days compared to AC with 76% (1036 ppm). Other lower adsorbent of treated samples BB1–4 and CBB adsorbed a relatively similar average of 62% net. The adsorption rate in all samples suggests that BC is a faster and better adsorbent material for Pb^{2+}. This result is contrary to Ramola et al. (2019), who observed that unmodified biochar, pyrolyzed at 700 °C, adsorbed less Pb^{2+} though with a bentonite calcite supplement amendment. However, there was no significant difference in Pb^{2+} sorption between BC, AC, treated BB1–4, and CBB samples (Kruskal-Wallis chi-squared = 1.3036, df = 2, p value = 0.5211).

3.2.2 Zn^{2+} Adsorption

The total net Zn^{2+} adsorption revealed that all the samples are suitable adsorbents but differed in sorption rates and capacity. At 1104-h final sampling interval, AC adsorbed 1221 ppm, BC 666 ppm, and lower sorption in other treated BB1–4 and CBB samples (Fig. 5). Zn^{2+} adsorption in AC was the most rapid compared to other adsorbents, which occurred at the first 72-h interval at 1.4 g/kg but rapidly underwent desorption afterward. Though AC was 3.2 folds higher than BC at 0.43 g/kg in the first 72-h sampling time, it was most unstable among other adsorbents. But there was no statistically significant difference in Zn^{2+} adsorption among all samples (Kruskal-Wallis chi-squared = 11.038, df = 6, p value = 0.08721).

Comparatively, Zn^{2+} adsorption between BC, AC, treated BB1–4, and CBB revealed that untreated AC was a better adsorbent with a statistically significant difference (Kruskal-Wallis chi-squared = 6.8, df = 2, p value = 0.03337). BB4, the least treated sample, was a better adsorbent than other treated samples by 28%. Among all samples, CBB was the least adsorbent (367 ppm) and had the lowest surface area but showed no statistical difference when compared with other treated samples (Kruskal-Wallis chi-squared = 2.3546, df = 4, p value = 0.6709). The total net Zn^{2+} adsorbed in this field setup by 50 g of each adsorbent in the 15.8 mg/L zinc concentration in 1104 h was 30 g/kg and 18 g/kg by AC and BC, respectively, in 0.014 m^3/s flow rate. In previous studies, different adsorbent materials have varied in their Zn^{2+} sorption capabilities. Biswas et al. (2019) recorded a maximum of 40.6 mg/g adsorption using

Table 3 Metal adsorption in all adsorbent samples

Hours	BC (ppm)	AC (ppm)	BB1 (ppm)	BB2 (ppm)	BB3 (ppm)	BB4 (ppm)	CBB (ppm)
Pb^{2+} (lead) adsorption							
72	239 ± 12.19	163 ± 7.07	216 ± 12.69	163 ± 10.84	169 ± 18.06	215 ± 12.26	75 ± 10.71
240	670 ± 15.44	522 ± 15.66	398 ± 9.05	482 ± 24.41	355 ± 13.54	359 ± 15.66	412 ± 23.54
432	916 ± 21.41	716 ± 13.25	476 ± 10.41	590 ± 21.83	566 ± 13.54	638 ± 17.41	334 ± 11.77
624	1065 ± 24.31	786 ± 8.34	588 ± 16.51	528 ± 12.12	664 ± 17.07	601 ± 17.64	591 ± 14.24
1104	1335 ± 28.49	1036 ± 17.07	910 ± 24.24	950 ± 14.24	937 ± 21.55	1264 ± 26.4	760 ± 14.83
Zn^{2+} (zinc) adsorption							
72	429 ± 11.20	1371 ± 10.56	559 ± 18.41	365 ± 10.34	321 ± 17.35	453 ± 14.10	218 ± 19.05
240	447 ± 14.10	1111 ± 16.51	313 ± 13.96	311 ± 10.78	215 ± 13.32	236 ± 10.20	209 ± 16.08
432	621 ± 13.82	953 ± 20.97	319 ± 14.84	468 ± 13.32	416 ± 19.40	407 ± 15.52	244 ± 20.49
624	510 ± 13.75	1021 ± 24.81	454 ± 22.40	296 ± 14.60	458 ± 10.78	374 ± 13.68	444 ± 15.23
1104	666 ± 22.97	1221 ± 17.42	469 ± 16.79	507 ± 23.25	523 ± 15.80	600 ± 11.24	367 ± 17.42

Comparative adsorption of Pb^{2+} and Zn^{2+} in all adsorbent samples of BC (untreated biochar), control AC (activated carbon), and BB1–4 (treated biophos ash to biochar samples of 1:10, 1:35, 1:50, 1:100) and CBB (treated biophos ash to cockleshell ash to biochar at ratios 1:1:100). Adsorption values are recorded as mean ± standard deviation for three replicated samples

Ca-alginate-biochar composite (CABC) adsorbent in a constant 50 mg/L concentration, while 7.48 mg/g and 4.98 mg/g were adsorbed using hardwood and corn straw, respectively, from 100 mM Cu(II) and Zn(II) stock solution (Chen et al. 2011).

In a batch experiment of Cu and Zn adsorption from a mine-contaminated water, Rodríguez-Vila et al. (2018) observed lesser Zn^{2+} adsorption in circumneutral mine discharged than the acid mine drain (AMD) water. This adsorption was attributed to a higher Zn^{2+} concentration of 14.16 mg/L than 8.98 mg/L in the circumneutral mine, which is slightly lower than Frongoch discharge at 15.8 mg/L concentration and 7.2 pH. Notwithstanding, these studies were carried out in laboratory conditions under a

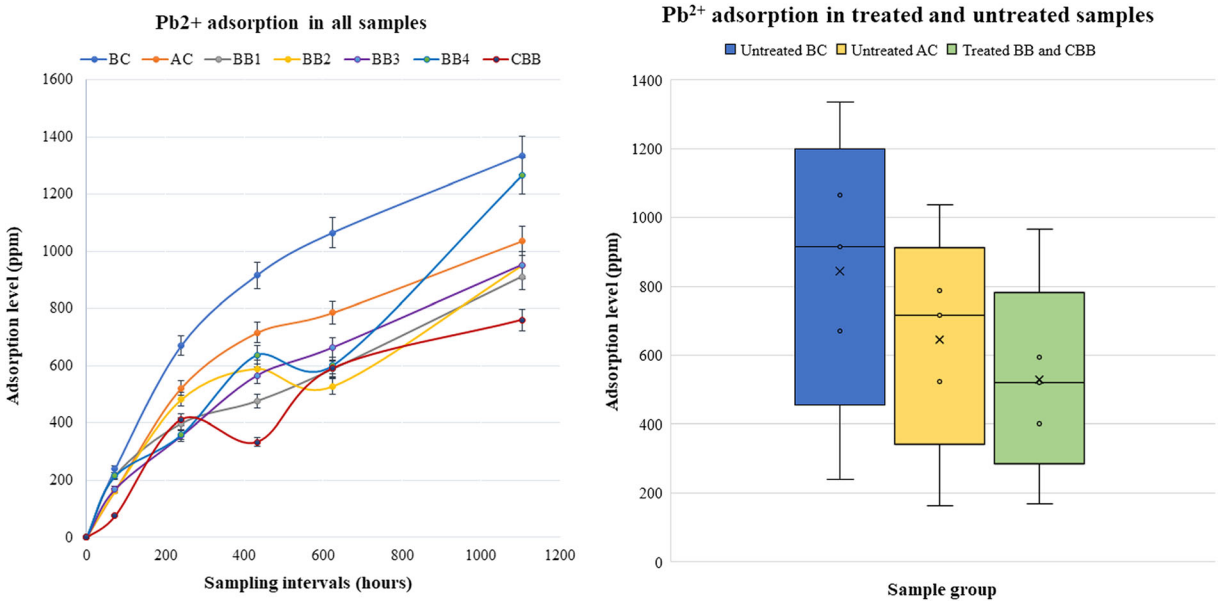

Fig. 3 **a** Pb^{2+} net absorption in 1104 h of sampling time and **b** comparative box-and-whiskers plot showing net adsorption differences between untreated biochar (BC), activated carbon (AC), and treated BB1–4 and CBB samples

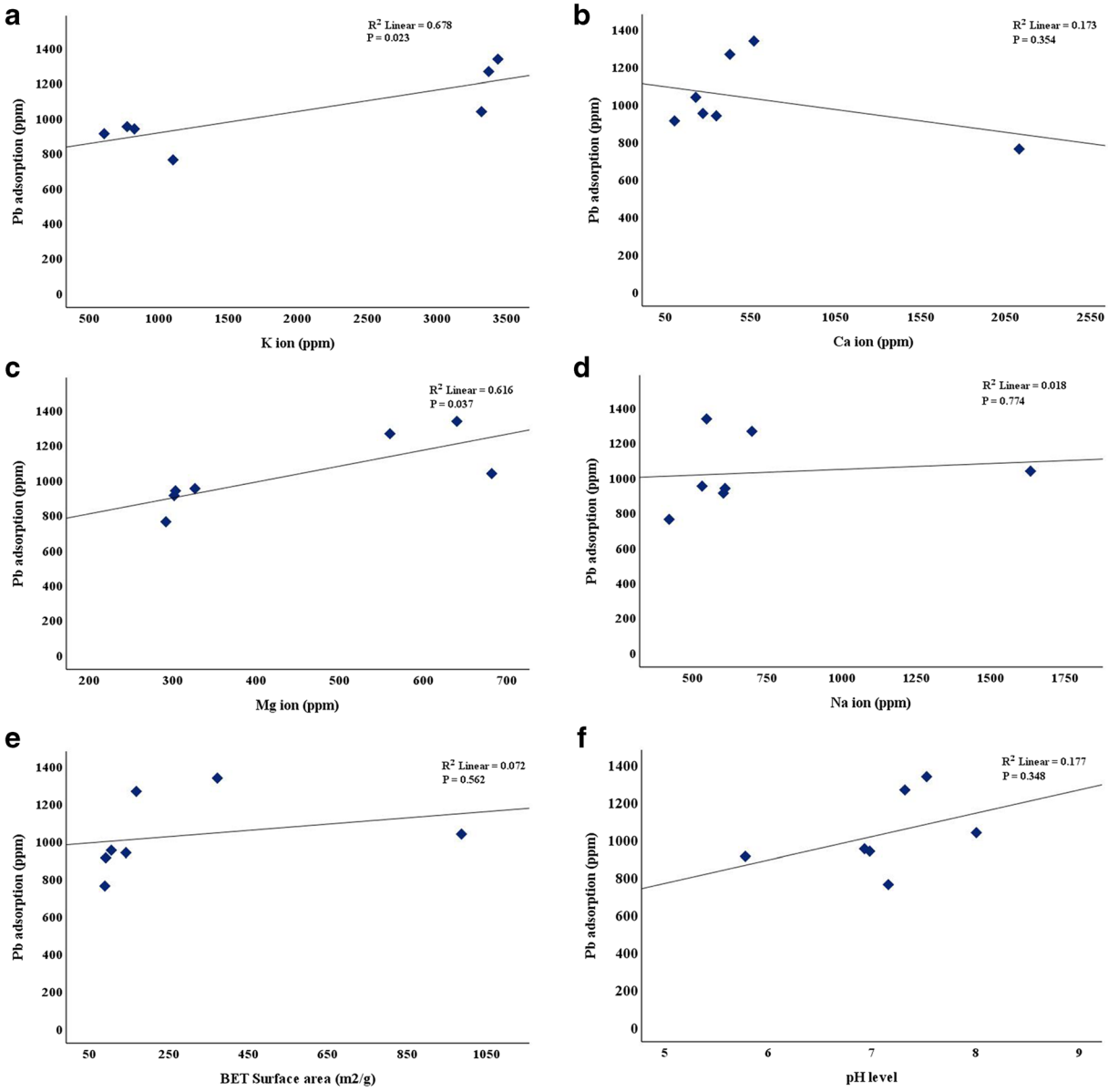

Fig. 4 Pb^{2+} adsorption correlations with adsorbent physicochemical properties. **a** K^+ ion. **b** Ca^{2+} ion. **c** Mg^{2+} ion. **d** Na^+ ion, **e** BET surface area. **f** pH level. Pearson's R^2 coefficients and significance (p) values indicated at 95% confidence level

constant metal concentration and not flowing water like Frongoch watercourse. Hence, the need for a field trial where adsorption conditions are not regulated is suggested.

The adsorptive correlation analysis suggests that Fe^{2+} content, Na^+ content, and surface area are possible mechanisms attributable to increased Zn^{2+} adsorption (Fig. 6a–f). The Fe^{2+} and Na^+ contents in AC were 4.4 and 3.0 folds, respectively, greater than BC and suggestive of the 0.6 g/kg higher Zn^{2+} adsorption in AC. A previous study by Jiang et al. (2015) observed significant differences in Zn^{2+} adsorption with changes in Na_2SO_4 concentrations, which revealed that Na^+ ion content enhanced Zn^{2+} adsorption. A similar attribute was observed in water hyacinth-activated biochar, where $FeCl_2$-activated biochar exhibited a robust magnetic property and adsorption capability observed through FTIR spectra (Nyamunda et al. 2019). The BET surface area was positively correlated with Pb^{2+} and Zn^{2+} adsorption, but most statistically ($p < 0.001$) correlated with Zn^{2+} adsorption due to a 90.5% higher surface area of AC than other samples. The high porosity and large surface

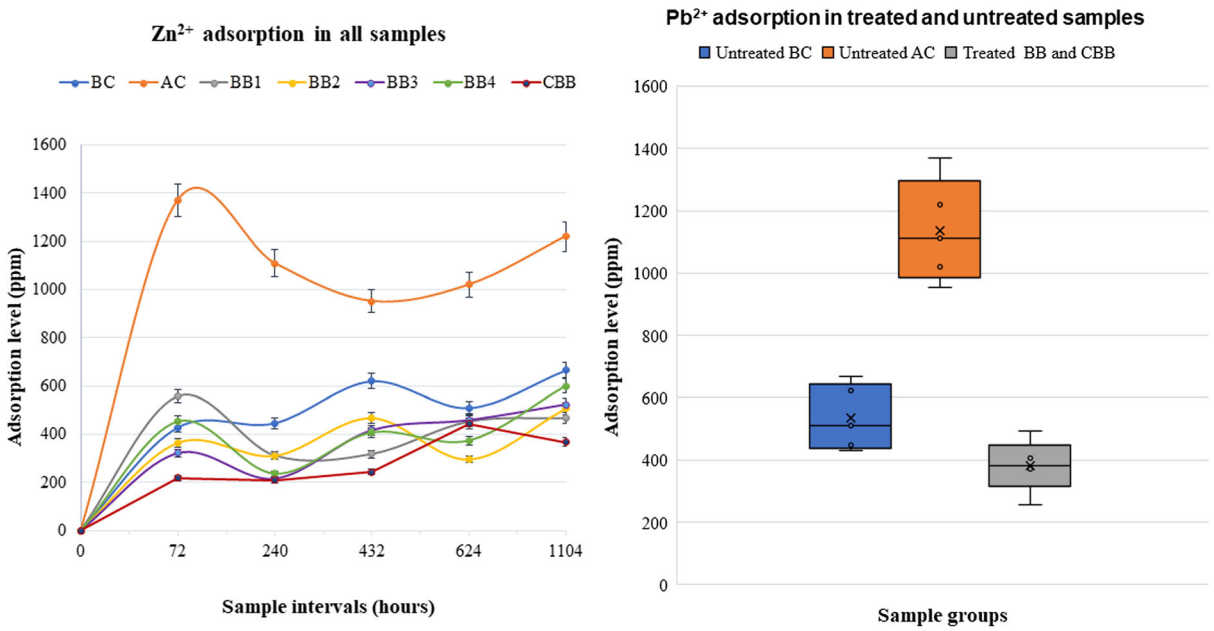

Fig. 5 **a** Zn^{2+} net absorption in 1104 h of sampling time and **b** comparative box-and-whiskers plot shows net adsorption differences between untreated biochar (BC), activated carbon (AC), treated BB1–4, and CBB samples

area of AC suggest to have increased adsorbent surface exposure for ion exchange and binding sites for heavy metals, which has been reported earlier (Chen et al. 2011; Jeyakumar and Chandrasekaran 2014; J. J. Zhao et al. 2019). In conformity with previous studies, Cibati et al. (2017) noted that commercial Norit AC was 1.9 times better than non-activated BC from Miscanthus biomass due to its 5.8 m^2/g greater BET surface area. These notable factors suggest that with a higher BET surface area and more significant Fe^{2+} binding sites, AC had adsorbed more Zn^{2+} than BC. In a batch and column test of mixed metals, Ding et al. (2016) achieved 1.83 mg/g Zn^{2+} removal in a mixed 100 mg/L metal solution of Zn^{2+}, Pb^{2+}, Cd^{2+}, Cu^{2+}, and Ni^{2+} in 140 min using an alkaline-modified biochar surface area (873 m^2/g). Xue et al. (2020) noted that in a medium where there is a competitive adsorption, the effect of adsorbed Pb^{2+} on biochar surface could also alter the sorption sites for Zn^{2+} on BC, while pH positively correlates with adsorption of both metals but not statistically significant, which is similar to this study.

3.3 Adsorption Equilibrium Over Time and Possible Adsorbent Modification to Optimize Sorption Capabilities

Comparative adsorption equilibrium between Pb^{2+} and Zn^{2+} at different intervals is based on the adsorption curve shown in Figs. 3 and 5. Pb^{2+} adsorption declined from 3.3 to 0.6 ppm/h in BC, while Zn^{2+} from 6.0 to 0.3 ppm/h between the first and last sampling intervals. These adsorption differences show that BC has more potential to sorb more Pb^{2+} than Zn^{2+}. The gradual sorption decrease towards equilibrium suggests an effect of surface coverage, which is described as a chemisorption surface factor by a rapid initial surface reaction followed by slow secondary accumulation (Betts et al. 2013; Xue et al. 2020). Moreover, Zn^{2+} adsorption was relatively inconsistent due to metal desorption intervals and occurred in all samples, but notable in the most treated sample with the least surface area. Conversely, AC had the highest surface area but most desorbed metal after the initial sampling interval and never regained its optimal sorbed Zn^{2+}. A regression analysis to decipher the adsorption relationship between Pb^{2+} and Zn^{2+} showed a positive correlation with treated and untreated biochar samples, while AC was inversely or negatively correlated (Fig. S1). Hence, it suggests a competitive surface adsorption effect amidst multiple metal ions (Pb, Zn, Al, Cd, Fe, Ni, Co, Cu, and Cr) present in the contaminated water. Thus, Pb^{2+} over Zn^{2+} on biochar surface than activated carbon was favored, as reported in a previous study (Bearcock et al. 2010).

Generally, biochar with large surface area and pore volumes can provide sufficient binding sites for heavy

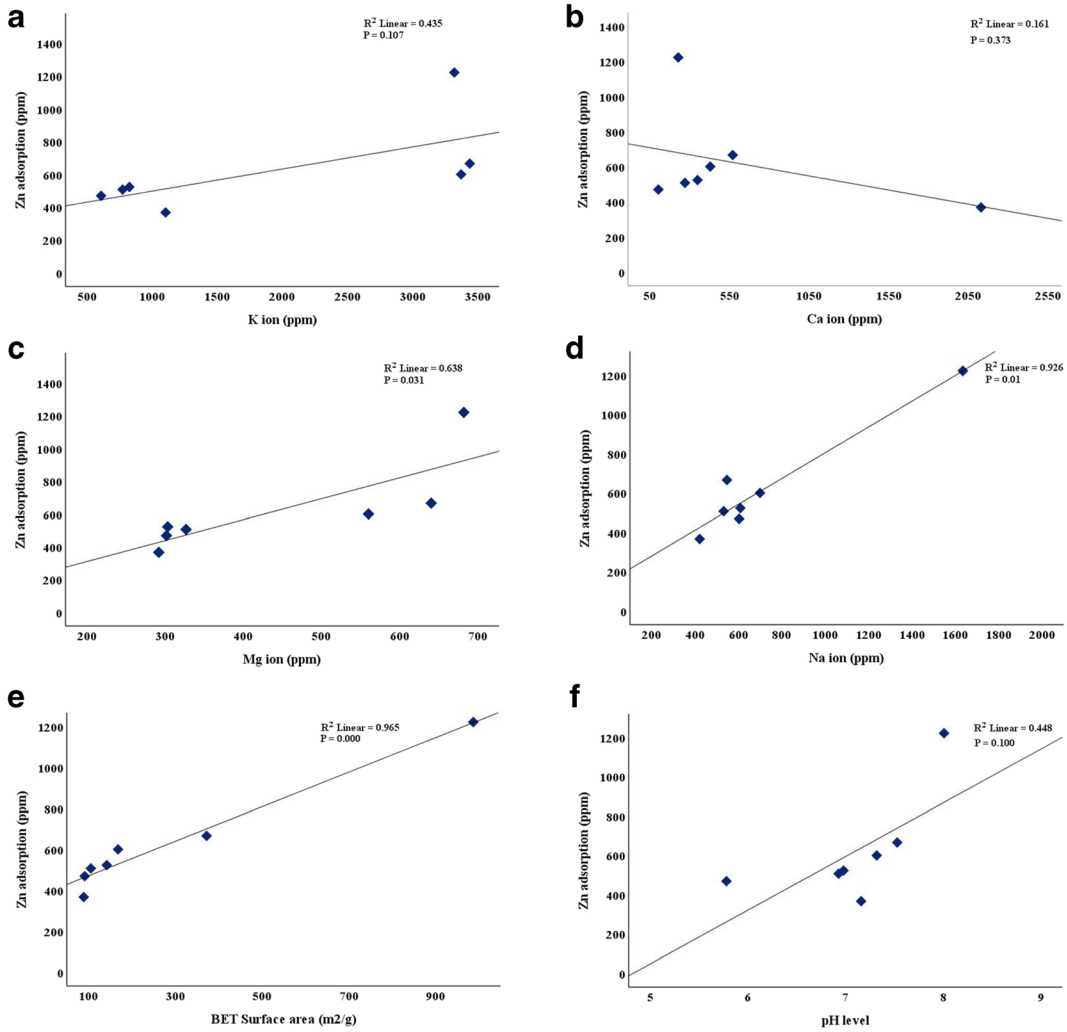

Fig. 6 Zn^{2+} adsorption correlations with adsorbents' physicochemical properties. **a** K^{+} ion. **b** Ca^{2+} ion. **c** Mg^{2+} ion. **d** Na^{+} ion. **e** BET surface area. **f** pH level. Pearson's R^2 coefficients and significance (p) values indicated at 95% confidence level

metals, otherwise subjected to competitive and inconsistent adsorption (J. H. Park et al. 2016). Among several studies of competitive metal adsorption in aqueous solution using various adsorbents (Ni et al. 2019; J. H. Park et al. 2015a, b; Sellaoui et al. 2019). J. H. Park et al. (2016) observed higher adsorption of Pb^{2+} in a multimetal aqueous solution containing Cu, Cr, Zn, and C, irrespective of the metals' electronegativity. This affinity was attributed to the smaller hydrated radius of Pb^{2+} (4.01 Å) compared to Zn^{2+} (4.30 Å), and more significant affinity to functional groups in the organic matter, which include phenolic and carboxylic groups. Other reported attributes include its higher atomic weight and radius, hydrolysis constant, and Misono softness value (J. H. Park et al. 2016). Sellaoui et al. (2019) also observed an antagonistic reduction in Zn^{2+} adsorption by 66% as well as 10% and 9.8% of Hg^{2+} and Pb^{2+} adsorption in Hg^{2+} and Pb^{2+} multi-metallic solution. The endothermic and competitive adsorption was explained by a density functional theory (DTF), which noted that atomic binding energies of metals contribute to adsorbent performance, depending on the ions present. Thus, by this study, Pb^{2+} sorption application using BC adsorbent in the Frongoch watercourse is recommended at an optimal sampling interval of 1104 h at 0.6 ppm/h and Zn^{2+} at 432 h (0.9 ppm/h), at a concentration of 0.62 mg/L and 0.014 m^3/s flow. Similarly, using AC adsorbent is recommended at 1104-h

interval at 0.5 ppm/h for Pb^{2+} adsorption while Zn^{2+} at 72 h (19.0 ppm/h).

3.3.1 Recommended Amendments for Optimal Sorption

The adsorbents' physicochemical properties and correlation with metal sorption show that ash amendment after pyrolysis altered the surface area necessary for metal binding. Therefore, it is suggestive of further trial applications for improvement. Firstly, by amendment process of biomass co-pyrolysis with ash. This co-amendment has recorded a successfully increased BET surface area of adsorbent biomass in previous studies (Z. Wang et al. 2019b; Ye et al. 2016). Furthermore, hydroxyl group modifications such as NaOH, KOH, NH_4OH, and HNO_3 before or after pyrolysis have been observed to improve porosity and surface area of biochar (Li et al. 2017; J.-H. Park et al. 2015a, b; Senthilkumar and Prasad 2020; X. Yang et al. 2019b). In a previous study, Ding et al. (2016) modified hickory wood biochar using alkaline (20 mL of 5 M NaOH) solution at 70 °C for 4 h to increase biochar surface area from 256 to 873 m^2/g and CEC from 45.7 to 124.5 cmol/kg. Indications of the surface functional group show that alkaline modification decreased the surface C from 86.7 to 57.9% while increased surface O from 12.0 to 33.3%, to yield an increased atomic ratio of surface O/C from 0.14 to 0.58. The alkaline (NaOH) modification increased the specific surface areas and binding energy of target heavy metal ions (Pb^{2+}, Cd^{2+}, Cu^{2+}, Zn^{2+}, and Ni^{2+}), which has also been recorded in most alkaline-modified studies (Cazetta et al. 2011; Uchimiya et al. 2011). Also, OH modification; Fe impregnation using alpha-FeOOH, alpha- and gamma-Fe_2O_3, $CuFe_2O_3$, $FeCl_2$, and $FeCl_3$; and saturation have been recorded in previous studies (Godlewska et al. 2020; Nyamunda et al. 2019; L. Yang et al. 2019a; T. Zhao et al. 2020). In a previous study, Nyamunda et al. (2019) saturated 200 g of dry water hyacinth biomass in a 1000 mL (2 M) mixture of $FeCl_2$ and $FeCl_3$ with an additional 5 M NaOH to increase its pH to 10 under rigorous magnetic stirring for 30 min. The modification increased its surface area from 610.88 to 1038 $m^2\ g^{-1}$ at 450 °C pyrolysis temperature. Nevertheless, due consideration to biomass type is recommended. A reconstruction of the installation pool site might be necessary to channel all contaminated mine water through the designed adsorbent biochar column for optimal sorption efficiency.

4 Conclusion

This study provides the opportunity to utilize low-cost adsorbent materials through pyrolysis of waste pinewood feedstock (*leylandii*) to limit the exposure pathway of Pb^{2+} and Zn^{2+} contamination from abandoned mines. The untreated BC and purchased activated biochar AC are better promising absorbents for minimizing Pb^{2+} and Zn^{2+} pollution. In 1104 h (46 days), a total net of 33 g/kg and 25 g/kg of Pb^{2+} was adsorbed using 50 g of BC and AC, respectively, while a total net of 30 g/kg and 18 g/kg of Zn^{2+} was adsorbed by AC and BC respectively.

Analysis of adsorption results revealed that adsorbent physicochemical properties such as K^+, Ca^{2+}, Mg^{2+}, Na^+, BET, and pH are primary mechanisms attributed to the differences in Pb^{2+} and Zn^{2+} adsorption. The BC samples contained 570.80 ppm Ca^{2+} and 640.72 ppm Mg^{2+} mineral ions which enhanced its surface for metal binding sites. More also, Fe^{2+} and Na^+ at 958.09 ppm and 1635.01 ppm in AC correlatively increased Zn^{2+} adsorption. High BET surface area enhanced metal adsorption mostly in untreated BC and AC samples, while post-ash amendment supplement significantly altered treated adsorbents' properties BB1–4 and CBB, notably the surface area, which provides binding sites for ion exchange.

Zn^{2+} metal desorption suggests the possibility of ion exchange by competitive adsorption, which slightly favored Pb^{2+} uptake in the multimetal-contaminated water by displacement interaction. Previous studies attributed similar ion exchange effect to electronegativity, a smaller hydrated radius of Pb^{2+}, and a more significant affinity to functional groups such as phenolic and carboxylic groups. Thus, it should be a factor to be considered in further studies.

Recommended modifications to improve adsorbent physicochemical properties include hydroxyl group modifications such as NaOH, KOH, NH_4OH, and HNO_3, before or after pyrolysis, and also OH modification and Fe impregnation using alpha-FeOOH, alpha- and gamma-Fe_2O_3, $CuFe_2O_3$, $FeCl_2$, and $FeCl_3$, as recorded in previous studies.

Supplementary Information The online version contains supplementary material available at https://doi.org/10.1007/s11270-021-05004-7.

Acknowledgments This research was supported by Mr. Sion, the director of the pyrolysis company Brackenbury of Commons Vision Ltd, who provided the ash. Tom Williams from Natural Resources Wales (NRW) for giving us access to the mine site, water quality testing, and the release of earlier monitoring data. Department of Bioscience Swansea University, where all the analysis was performed. Professor Alayne Street-Perrott, a co-supervisor of this research project. The Tertiary Education Trust Fund (TETFund) Nigeria provided the study sponsorship through the Federal College of Education (Technical) Omoku.

References

Amari, A., Alalwan, B., Eldirderi, M. M., Mnif, W., & Ben Rebah, F. (2019). Cactus material-based adsorbents for the removal of heavy metals and dyes: a review. *Materials Research Express*. https://doi.org/10.1088/2053-1591/ab5f32.

ASTM D6851. (2011). Standard test method for determination of contact pH with activated carbon (ASTM D6851). In *American Standard Test Method* (p. 5). https://doi.org/10.1520/d6851-02r11.

Bearcock, J., Palumbo-Roe, B., Banks, V., & Klinck, B. (2010). The hydrochemistry of Frongoch Mine, mid Wales. British Geological Survey. http://nora.nerc.ac.uk/12302/

Bentley, M. J., & Summers, R. S. (2020). Ash pretreatment of pine and biosolids produces biochars with enhanced capacity for organic micropollutant removal from surface water, wastewater, and stormwater. *Environmental Science: Water Research & Technology, 6*(3), 635–644. https://doi.org/10.1039/c9ew00862d.

Betts, A. R., Chen, N., Hamilton, J. G., & Peak, D. (2013). Rates and mechanisms of Zn2+ adsorption on a meat and bonemeal biochar. *Environmental Science and Technology, 47*(24), 14350–14357. https://doi.org/10.1021/es4032198.

Biswas, S., Sen, T. K., Yeneneh, A. M., & Meikap, B. C. (2019). Synthesis and characterization of a novel Ca-alginate-biochar composite as efficient zinc (Zn 2+) adsorbent: thermodynamics, process design, mass transfer and isotherm modeling. *Separation Science and Technology (Philadelphia), 54*(7), 1106–1124. https://doi.org/10.1080/01496395.2018.1527353.

Biswas, S., Siddiqi, H., Meikap, B. C., Sen, T. K., & Khiadani, M. (2020). Preparation and characterization of raw and inorganic acid-activated pine cone biochar and its application in the removal of aqueous-phase Pb2+ metal ions by adsorption. *Water, Air, and Soil Pollution, 231*(1), 7. https://doi.org/10.1007/s11270-019-4375-7.

Boeykens, S. P., Redondo, N., Obeso, R. A., Caracciolo, N., & Vázquez, C. (2019). Chromium and lead adsorption by avocado seed biomass study through the use of total reflection x-ray fluorescence analysis. *Applied Radiation and Isotopes, 153*, 108809. https://doi.org/10.1016/j.apradiso.2019.108809.

Budin, K., Subramaniam, Y., Tair, R., & Mohd Ali, S. A. (2014). springer. *IOSR Journal of Environmental Science, Toxicology and Food Technology, 8*(12), 04–06. https://doi.org/10.9790/2402-081210406.

Cazetta, A. L., Vargas, A. M. M., Nogami, E. M., Kunita, M. H., Guilherme, M. R., Martins, A. C., et al. (2011). NaOH-activated carbon of high surface area produced from coconut shell: kinetics and equilibrium studies from the methylene blue adsorption. *Chemical Engineering Journal, 174*(1), 117–125. https://doi.org/10.1016/j.cej.2011.08.058.

Chen, X., Chen, G., Chen, L., Chen, Y., Lehmann, J., McBride, M. B., & Hay, A. G. (2011). Adsorption of copper and zinc by biochars produced from pyrolysis of hardwood and corn straw in aqueous solution. *Bioresource Technology, 102*(19), 8877–8884. https://doi.org/10.1016/J.BIORTECH.2011.06.078.

Cheung, C. W., Porter, J. F., & McKay, G. (2000). Sorption kinetics for the removal of copper and zinc from effluents using bone char. *Separation and Purification Technology, 19*(1–2), 55–64. https://doi.org/10.1016/S1383-5866(99)00073-8.

Chi, T., Zuo, J., & Liu, F. (2017). Performance and mechanism for cadmium and lead adsorption from water and soil by corn straw biochar. *Frontiers of Environmental Science & Engineering, 11*(2). https://doi.org/10.1007/s11783-017-0921-y.

Cibati, A., Foereid, B., Bissessur, A., & Hapca, S. (2017). Assessment of Miscanthus × giganteus derived biochar as copper and zinc adsorbent: study of the effect of pyrolysis temperature, pH and hydrogen peroxide modification. *Journal of Cleaner Production, 162*, 1285–1296. https://doi.org/10.1016/j.jclepro.2017.06.114.

Crane, R. A., Sinnett, D. E., Cleall, P. J., & Sapsford, D. J. (2017). Physicochemical composition of wastes and co-located environmental designations at legacy mine sites in the south west of England and Wales: implications for their resource potential. *Resources, Conservation and Recycling, 123*, 117–134. https://doi.org/10.1016/j.resconrec.2016.08.009.

Ding, Z., Hu, X., Wan, Y., Wang, S., & Gao, B. (2016). Removal of lead , copper , cadmium , zinc , and nickel from aqueous solutions by alkali-modified biochar : batch and column tests. *Journal of Industrial and Engineering Chemistry, 33*, 239–245.

Edwards, P., & Williams, T. (2016). Abandoned mine case study: Frongoch Lead Mine. Natural Resources Wales. https://naturalresources.wales/media/679803/frongoch-mine-case-study_2016_06.pdf

Edwards, P., Williams, T., & Stanley, P. (2016). Surface water management and encapsulation of mine waste to reduce water pollution from Frongoch Mine, Mid Wales. In M. Drebenstedt & P. Carsten (Eds.), *Mining Meets Water – Conflicts and Solutions* (pp. 546–553). IMWA Proceedings: Freiberg/Germany http://www.mwen.info/docs/imwa_2016/IMWA2016_Edwards_46.pdf.

Environment Agency. (2012). *Future management of abandoned non-coal mine water discharges*. Bristol, UK: Environment Agency www.environment-agency.gov.uk.

Esrafili, A., Bagheri, S., Kermani, M., Gholami, M., & Moslemzadeh, M. (2019). Simultaneous adsorption of heavy metal ions (Cu2+ and Cd2+) from aqueous solutions by magnetic silica nanoparticles (Fe3O4@SiO2) modified using edta. *Desalination and Water Treatment, 158*(July), 207–215. https://doi.org/10.5004/dwt.2019.24274.

European Commission DG ENV. (2002). *Heavy metals in waste. Department for Environment, Food & Rural Affairs*. Denmark: COWI A/S.

Fahmi, A. H., Samsuri, A. W., Jol, H., & Singh, D. (2018). Physical modification of biochar to expose the inner pores and their functional groups to enhance lead adsorption. *RSC Advances, 8*(67), 38270–38280. https://doi.org/10.1039/c8ra06867d.

Foong, S. Y., Liew, R. K., Yang, Y., Cheng, Y. W., Yek, P. N. Y., Wan Mahari, W. A., et al. (2020). Valorization of biomass waste to engineered activated biochar by microwave pyrolysis: progress, challenges, and future directions. *Chemical Engineering Journal, 389*, 124401. https://doi.org/10.1016/j.cej.2020.124401.

Godlewska, P., Bogusz, A., Dobrzyńska, J., Dobrowolski, R., & Oleszczuk, P. (2020). Engineered biochar modified with iron as a new adsorbent for treatment of water contaminated by selenium. *Journal of Saudi Chemical Society*, 824–834. https://doi.org/10.1016/j.jscs.2020.07.006.

Godwin, P. M., Pan, Y., Xiao, H., & Afzal, M. T. (2019). Progress in preparation and application of modified biochar for improving heavy metal ion removal from wastewater. *Journal of Bioresources and Bioproducts, 4*(1), 31–42. https://doi.org/10.21967/JBB.V4I1.180.

Gyamfi, E., Appiah-Adjei, E. K., & Adjei, K. A. (2019). Potential heavy metal pollution of soil and water resources from artisanal mining in Kokoteasua, Ghana. *Groundwater for Sustainable Development, 8*(February), 450–456. https://doi.org/10.1016/j.gsd.2019.01.007.

Holguera, J. G., Etui, I. D., Jensen, L. H. S., & Peña, J. (2018). Contaminant loading and competitive access of Pb, Zn and Mn(III) to vacancy sites in biogenic MnO2. *Chemical Geology, 502*(October), 76–87. https://doi.org/10.1016/j.chemgeo.2018.10.020.

Hu, R., Xiao, J., Wang, T., Chen, G., Chen, L., & Tian, X. (2020). Engineering of phosphate-functionalized biochars with highly developed surface area and porosity for efficient and selective extraction of uranium. *Chemical Engineering Journal, 379*, 122388. https://doi.org/10.1016/J.CEJ.2019.122388.

Hudson, E., Kulessa, B., Edwards, P., Williams, T., & Walsh, R. (2018). Integrated hydrological and geophysical characterisation of surface and subsurface water contamination at abandoned metal mines. *Water, Air, and Soil Pollution, 229*(8). https://doi.org/10.1007/s11270-018-3880-4.

Inyang, M. I., Gao, B., Yao, Y., Xue, Y., Zimmerman, A., Mosa, A., et al. (2016). A review of biochar as a low-cost adsorbent for aqueous heavy metal removal. *Critical Reviews in Environmental Science and Technology, 46*(4), 406–433. https://doi.org/10.1080/10643389.2015.1096880.

Järup, L. (2003). Hazards of heavy metal contamination. *British Medical Bulletin, 68*, 167–182. https://doi.org/10.1093/bmb/ldg032.

Jarvis, A. P., & Mayes, W. M. (2012). *Prioritisation of abandoned non-coal mine impacts on the environment: hazards and risk management at abandoned non-coal sites*. Bristol: Department for Environmental food and rural affairs. https://doi.org/10.13140/2.1.2024.1440.

Jeyakumar, R. P. S., & Chandrasekaran, V. (2014). Adsorption of lead (II) ions by activated carbons prepared from marine green algae: equilibrium and kinetics studies. *International Journal of Industrial Chemistry, 5*(1), 1–9. https://doi.org/10.1007/s40090-014-0010-z.

Jiang, S., Huang, L., Nguyen, T. A. H., Ok, Y. S., Rudolph, V., Yang, H., & Zhang, D. (2015). Copper and zinc adsorption by softwood and hardwood biochars under elevated sulphate-induced salinity and acidic pH conditions. *Chemosphere*. https://doi.org/10.1016/j.chemosphere.2015.06.079.

Kim, Y., Oh, J.-I., Vithanage, M., Park, Y.-K., Lee, J., & Kwon, E. E. (2019). Modification of biochar properties using CO2. *Chemical Engineering Journal, 372*, 383–389. https://doi.org/10.1016/J.CEJ.2019.04.170.

Kwak, J. H., Islam, M. S., Wang, S., Messele, S. A., Naeth, M. A., El-Din, M. G., & Chang, S. X. (2019). Biochar properties and lead(II) adsorption capacity depend on feedstock type, pyrolysis temperature, and steam activation. *Chemosphere, 231*, 393–404. https://doi.org/10.1016/j.chemosphere.2019.05.128.

Lehmann, J., & Joseph, S. (2009). Biochar for environmental management. *Science and Technology, 1*, 449. https://doi.org/10.4324/9781849770552.

Li, H., Dong, X., da Silva, E. B., de Oliveira, L. M., Chen, Y., & Ma, L. Q. (2017). Mechanisms of metal sorption by biochars: biochar characteristics and modifications. *Chemosphere, 178*, 466–478. https://doi.org/10.1016/j.chemosphere.2017.03.072.

Liu, J., Huang, Z., Chen, Z., Sun, J., Gao, Y., & Wu, E. (2020). Resource utilization of swine sludge to prepare modified biochar adsorbent for the efficient removal of Pb(II) from water. *Journal of Cleaner Production, 257*(Ii), 120322. https://doi.org/10.1016/j.jclepro.2020.120322.

Liu, L., Huang, Y., Zhang, S., Gong, Y., Su, Y., Cao, J., & Hu, H. (2019). Adsorption characteristics and mechanism of Pb(II) by agricultural waste-derived biochars produced from a pilot-scale pyrolysis system. *Waste Management, 100*, 287–295. https://doi.org/10.1016/j.wasman.2019.08.021.

Liu, Z., & Zhang, F. S. (2009). Removal of lead from water using biochars prepared from hydrothermal liquefaction of biomass. *Journal of Hazardous Materials, 167*(1–3), 933–939. https://doi.org/10.1016/j.jhazmat.2009.01.085.

Loganathan, P., Shim, W. G., Sounthararajah, D. P., Kalaruban, M., Nur, T., & Vigneswaran, S. (2018). Modelling equilibrium adsorption of single, binary, and ternary combinations of Cu, Pb, and Zn onto granular activated carbon. *Environmental Science and Pollution Research, 25*(17), 16664–16675. https://doi.org/10.1007/s11356-018-1793-9.

Ma, Y., Liu, D. L., Schwenke, G., & Yang, B. (2019). The global warming potential of straw-return can be reduced by application of straw-decomposing microbial inoculants and biochar in rice-wheat production systems. *Environmental Pollution, 252*, 835–845. https://doi.org/10.1016/j.envpol.2019.06.006.

Mahdi, Z., Yu, Q. J., & El Hanandeh, A. (2018). Removal of lead(II) from aqueous solution using date seed-derived biochar: batch and column studies. *Applied Water Science, 8*(6), 1–13. https://doi.org/10.1007/s13201-018-0829-0.

Moideen, S. N. F., Din, M. F. M., Rezania, S., Ponraj, M., Rahman, A. A., Pei, L. W., et al. (2020). Dual phase role of composite adsorbents made from cockleshell and natural zeolite in treating river water. *Journal of King Saud University - Science, 32*(1), 1–6. https://doi.org/10.1016/j.jksus.2017.06.001.

Ni, B. J., Huang, Q. S., Wang, C., Ni, T. Y., Sun, J., & Wei, W. (2019). Competitive adsorption of heavy metals in aqueous solution onto biochar derived from anaerobically digested

sludge. *Chemosphere, 219*, 351–357. https://doi.org/10.1016/j.chemosphere.2018.12.053.

Novais, R. M., Buruberri, L. H., Seabra, M. P., & Labrincha, J. A. (2016). Novel porous fly-ash containing geopolymer monoliths for lead adsorption from wastewaters. *Journal of Hazardous Materials, 318*, 631–640. https://doi.org/10.1016/j.jhazmat.2016.07.059.

Nyamunda, B. C., Chivhanga, T., Guyo, U., & Chigondo, F. (2019). Removal of Zn (II) and Cu (II) ions from industrial wastewaters using magnetic biochar derived from water hyacinth. *Journal of Engineering (United Kingdom), 2019*, 983. https://doi.org/10.1155/2019/5656983.

Park, J.-H., Ok, Y. S., Kim, S.-H., Cho, J.-S., Heo, J.-S., Delaune, R. D., & Seo, D.-C. (2015a). Competitive adsorption of heavy metals onto sesame straw biochar in aqueous solutions. *Chemosphere*. https://doi.org/10.1016/j.chemosphere.2015.05.093.

Park, J. H., Cho, J. S., Ok, Y. S., Kim, S. H., Kang, S. W., Choi, I. W., et al. (2015b). Competitive adsorption and selectivity sequence of heavy metals by chicken bone-derived biochar: batch and column experiment. *Journal of Environmental Science and Health - Part A Toxic/Hazardous Substances and Environmental Engineering, 50*(11), 1194–1204. https://doi.org/10.1080/10934529.2015.1047680.

Park, J. H., Ok, Y. S., Kim, S. H., Cho, J. S., Heo, J. S., Delaune, R. D., & Seo, D. C. (2016). Competitive adsorption of heavy metals onto sesame straw biochar in aqueous solutions. *Chemosphere, 142*, 77–83. https://doi.org/10.1016/j.chemosphere.2015.05.093.

Paul Edwards. (2010). Frongoch Mine. Abandoned Metal Mines in Mid Wales. http://www.aspectsofwales.co.uk/gallery_frongoch_pre2011a.htm

Qiu, B., & Duan, F. (2019). Synthesis of industrial solid wastes/biochar composites and their use for adsorption of phosphate: from surface properties to sorption mechanism. *Colloids and Surfaces A: Physicochemical and Engineering Aspects, 571*, 86–93. https://doi.org/10.1016/J.COLSURFA.2019.03.041.

Rabia, A. R., Ibrahim, A. H., & Zulkepli, N. N. (2018). Activated alumina preparation and characterization: the review on recent advancement. In *E3S Web of Conferences* (Vol. 34, pp. 1–8). https://doi.org/10.1051/e3sconf/20183402049.

Ramola, S., Belwal, T., Li, C. J., Wang, Y. Y., Lu, H. H., Yang, S. M., & Zhou, C. H. (2019). Improved lead removal from aqueous solution using novel porous bentonite - and calcite-biochar composite. *Science of the Total Environment, 709*, 136171. https://doi.org/10.1016/j.scitotenv.2019.136171.

Renu, Agarwal, M., & Singh, K. (2017). Heavy metal removal from wastewater using various adsorbents: a review. *Journal of Water Reuse and Desalination*. https://doi.org/10.2166/wrd.2016.104.

Rodríguez-Vila, A., Selwyn-Smith, H., Enunwa, L., Smail, I., Covelo, E. F., & Sizmur, T. (2018). Predicting Cu and Zn sorption capacity of biochar from feedstock C/N ratio and pyrolysis temperature. *Environmental Science and Pollution Research, 25*(8), 7730–7739. https://doi.org/10.1007/s11356-017-1047-2.

Sellaoui, L., Mendoza-Castillo, D. I., Reynel-Ávila, H. E., Ávila-Camacho, B. A., Díaz-Muñoz, L. L., Ghalla, H., et al. (2019). Understanding the adsorption of Pb2+, Hg2+ and Zn2+ from aqueous solution on a lignocellulosic biomass char using advanced statistical physics models and density functional theory simulations. *Chemical Engineering Journal, 365*(January), 305–316. https://doi.org/10.1016/j.cej.2019.02.052.

Senthilkumar, R., & Prasad, D. M. R. (2020). Sorption of heavy metals onto biochar, applications of biochar for environmental safety. *IntechOpen, 13*. https://doi.org/10.5772/intechopen.92346.

Shi, P., Jing, H., & Xi, S. (2019). Urinary metal/metalloid levels in relation to hypertension among occupationally exposed workers. *Chemosphere, 234*, 640–647. https://doi.org/10.1016/J.CHEMOSPHERE.2019.06.099.

Song, J., Zhang, S., Li, G., Du, Q., & Yang, F. (2020). Preparation of montmorillonite modified biochar with various temperatures and their mechanism for Zn ion removal. *Journal of Hazardous Materials, 391*, 121692. https://doi.org/10.1016/j.jhazmat.2019.121692.

Tan, X., Liu, Y., Gu, Y., Xu, Y., Zeng, G., Hu, X., et al. (2016). Biochar-based nano-composites for the decontamination of wastewater: a review. *Bioresource Technology, 212*, 318–333. https://doi.org/10.1016/J.BIORTECH.2016.04.093.

Thompson, K. A., Shimabuku, K. K., Kearns, J. P., Knappe, D. R. U., Summers, R. S., & Cook, S. M. (2016). Environmental comparison of biochar and activated carbon for tertiary wastewater treatment. *Environmental Science and Technology, 50*(20), 11253–11262. https://doi.org/10.1021/acs.est.6b03239.

Uchimiya, M., Chang, S. C., & Klasson, K. T. (2011). Screening biochars for heavy metal retention in soil: role of oxygen functional groups. *Journal of Hazardous Materials, 190*(1–3), 432–441. https://doi.org/10.1016/j.jhazmat.2011.03.063.

Wang, H., Wang, H., Zhao, H., & Yan, Q. (2020). Adsorption and Fenton-like removal of chelated nickel from Zn-Ni alloy electroplating wastewater using activated biochar composite derived from Taihu blue algae. *Chemical Engineering Journal, 379*(July 2019), 122372. https://doi.org/10.1016/j.cej.2019.122372.

Wang, L., Wang, Y., Ma, F., Tankpa, V., Bai, S., Guo, X., & Wang, X. (2019a). Mechanisms and reutilization of modified biochar used for removal of heavy metals from wastewater: a review. *Science of the Total Environment, 668*, 1298–1309. https://doi.org/10.1016/j.scitotenv.2019.03.011.

Wang, S., Soudi, M., Li, L., & Zhu, Z. H. (2006). Coal ash conversion into effective adsorbents for removal of heavy metals and dyes from wastewater. *Journal of Hazardous Materials, 133*(1–3), 243–251. https://doi.org/10.1016/j.jhazmat.2005.10.034.

Wang, S., Gao, B., Zimmerman, A. R., Li, Y., Ma, L., Harris, W. G., & Migliaccio, K. W. (2015). Physicochemical and sorptive properties of biochars derived from woody and herbaceous biomass. *Chemosphere, 134*, 257–262. https://doi.org/10.1016/j.chemosphere.2015.04.062.

Wang, Y., & Liu, R. (2017). Comparison of characteristics of twenty-one types of biochar and their ability to remove multi-heavy metals and methylene blue in solution. *Fuel Processing Technology, 160*, 55–63. https://doi.org/10.1016/j.fuproc.2017.02.019.

Wang, Z., Xie, L., Liu, K., Wang, J., Zhu, H., Song, Q., & Shu, X. (2019b). Co-pyrolysis of sewage sludge and cotton stalks. *Waste Management, 89*, 430–438. https://doi.org/10.1016/j.wasman.2019.04.033.

WHO. (2011). *Guidelines for drinking-water quality*, *World Health Organization (Fourth.)*. Geneva: WHO Press. https://doi.org/10.1007/978-1-4020-4410-6_184.

Wu, Q., Xian, Y., He, Z., Zhang, Q., Wu, J., Yang, G., et al. (2019). Adsorption characteristics of Pb(II) using biochar derived from spent mushroom substrate. *Scientific Reports, 9*(1), 1–11. https://doi.org/10.1038/s41598-019-52554-2.

Xiao, R., Wang, P., Mi, S., Ali, A., Liu, X., Li, Y., et al. (2019). Effects of crop straw and its derived biochar on the mobility and bioavailability in Cd and Zn in two smelter-contaminated alkaline soils. *Ecotoxicology and Environmental Safety, 181*(February), 155–163. https://doi.org/10.1016/j.ecoenv.2019.06.005.

Xiao, Y., Xue, Y., Gao, F., & Mosa, A. (2017). Sorption of heavy metal ions onto crayfish shell biochar: effect of pyrolysis temperature, pH and ionic strength. *Journal of the Taiwan Institute of Chemical Engineers, 80*, 114–121. https://doi.org/10.1016/J.JTICE.2017.08.035.

Xu, L., Cui, H., Zheng, X., Liang, J., Xing, X., Yao, L., et al. (2018). Adsorption of Cu2+ to biomass ash and its modified product. *Water Science and Technology, 2017*(1), 115–125. https://doi.org/10.2166/wst.2018.095.

Xue, C., Zhu, L., Lei, S., Liu, M., Hong, C., Che, L., et al. (2020). Lead competition alters the zinc adsorption mechanism on animal-derived biochar. *Science of the Total Environment, 713*, 136395. https://doi.org/10.1016/j.scitotenv.2019.136395.

Yang, L., He, L., Xue, J., Wu, L., Ma, Y., Li, H., et al. (2019a). Highly efficient nickel (II) removal by sewage sludge biochar supported α-Fe2O3 and α-FeOOH: sorption characteristics and mechanisms. *PLoS One, 14*(6), 1–16. https://doi.org/10.1371/journal.pone.0218114.

Yang, X., Zhang, S., Ju, M., & Liu, L. (2019b). Preparation and modification of biochar materials and their application in soil remediation. *Applied Sciences (Switzerland).* https://doi.org/10.3390/app9071365.

Yargicoglu, E. N., & Reddy, K. R. (2014). Evaluation of PAH and metal contents of different biochars for use in climate change mitigation systems. In *American Society of Civil Engineers* (pp. 114–126). https://doi.org/10.1061/9780784478745.011.

Ye, C., Yang, X., Zhao, F.-J., & Ren, L. (2016). The shift of the microbial community in activated sludge with calcium treatment and its implication to sludge settleability. *Bioresource Technology, 207*, 11–18. https://doi.org/10.1016/J.BIORTECH.2016.01.135.

Yu, J., Xiong, W., Sun, Q., Zhu, J., Chi, R., & Zhang, Y. (2019). Separation of Pb2+ from Mg2+ by modified sugarcane bagasse under batch and column conditions: effect of initial concentration ratio. *Arabian Journal of Chemistry, 12*(8), 4438–4445. https://doi.org/10.1016/J.ARABJC.2016.07.005.

Zhang, J., Shao, J., Jin, Q., Li, Z., Zhang, X., Chen, Y., et al. (2019). Sludge-based biochar activation to enhance Pb(II) adsorption. *Fuel, 252*, 101–108. https://doi.org/10.1016/J.FUEL.2019.04.096.

Zhang, T., Zhu, X., Shi, L., Li, J., Li, S., Lü, J., & Li, Y. (2017). Efficient removal of lead from solution by celery-derived biochars rich in alkaline minerals. *Bioresource Technology, 235*, 185–192. https://doi.org/10.1016/j.biortech.2017.03.109.

Zhang, W., Du, W., Wang, F., Xu, H., Zhao, T., Zhang, H., et al. (2020). Comparative study on Pb2+ removal from aqueous solutions using biochars derived from cow manure and its vermicompost. *Science of the Total Environment, 716*, 137108. https://doi.org/10.1016/j.scitotenv.2020.137108.

Zhang, Z., Wang, X., Wang, Y., Xia, S., Chen, L., Zhang, Y., & Zhao, J. (2013). Pb(II) removal from water using Fe-coated bamboo charcoal with the assistance of microwaves. *Journal of Environmental Sciences (China), 25*(5), 1044–1053. https://doi.org/10.1016/S1001-0742(12)60144-2.

Zhao, J. J., Shen, X. J., Domene, X., Alcañiz, J. M., Liao, X., & Palet, C. (2019). Comparison of biochars derived from different types of feedstock and their potential for heavy metal removal in multiple-metal solutions. *Scientific Reports, 9*(1), 1–12. https://doi.org/10.1038/s41598-019-46234-4.

Zhao, T., Ma, X., Cai, H., Ma, Z., & Liang, H. (2020). Study on the adsorption of CuFe2O4-loaded corncob biochar for Pb(II). *Molecules, 25*(15). https://doi.org/10.3390/molecules25153456.